Geomechanics and Engineering, *Vol. 34, No. 5 (2023) 491-505*
https://doi.org/10.12989/gae.2023.34.5.491

Stability of rectangular tunnel in improved soil surrounded by soft clay

Siddharth Pandey[a] and Akanksha Tyagi*

Department of Civil Engineering, Indian Institute of Technology Roorkee, India, 247667

(*Received July 26, 2022, Revised July 23, 2023, Accepted July 24, 2023*)

Abstract. The practical usage of underground space and demand for vehicular tunnels necessitate the construction of non-circular wide rectangular tunnels. However, constructing large tunnels in soft clayey soil conditions with no ground improvement can lead to excessive ground deformations and collapse. In recent years, in situ ground improvement techniques such as jet grouting and deep cement mixing are often utilized to perform cement-stabilisation around the tunnel boundary to prevent large deformations and failure. This paper discusses the stability characteristics and failure behaviour of a wide rectangular tunnel in cement-treated soft clays. First, the plane strain finite element model is developed and validated with the results of centrifuge model tests available in the past literature. The critical tunnel support pressures computed from the numerical study are found to be in good agreement with those of centrifuge model tests. The influence of varying strength and thickness of improved soil surround, and cover depth are studied on the stability and failure modes of a rectangular tunnel. It is observed that the failure behaviour of the tunnel in improved soil surround depends on the ratio of the strength of improved soil surround to the strength of surrounding soil, i.e., q_{ui}/q_{us}, rather than just q_{ui}. For low q_{ui}/q_{us} ratios, the stability increases with the cover; however, for the high strength improved soil surrounds with $q_{ui} >> q_{us}$, the stability decreases with the cover. The failure chart, modified stability equation, and stability chart are also proposed as preliminary design guidelines for constructing rectangular tunnels in the improved soil surrounded by soft clays.

Keywords: cement-treated clays; cover; failure behaviour; rectangular tunnel; stability

1. Introduction

Tunnelling in soft soils is a challenging task that may often lead to the formation of sinkholes and even collapse. Numerous researchers have studied the undrained stability of circular tunnels in clayey soils (Mair 1979, Davis *et al*. 1980, Casarin and Mair 1981, Lee *et al*. 2006). There are numerous studies on the stability of circular tunnels in layered soils (Khezri *et al*. 2016, Yang and Zhang 2017).

The effective utilization of underground space and non-circular transportation modes such as vehicles and trains, necessitates the demand for non-circular tunnel geometry, for example, square and wide rectangle. In recent years, the construction of large non-circular tunnels has increased rapidly worldwide; some examples can be seen in Table 1.

Numerous studies have been done on the stability of square tunnels in soft clays (Assadi and Sloan 1991, Sloan and Assadi 1991), and cohesive-frictional soils (Layamin *et al*. 2001, Yamamoto *et al*. 2011). Uktritchon and Keawsawasvong (2020) studied the stability of square tunnels in clays with linearly increasing anisotropic shear strength. Yang and Yang (2010) and Zhang *et al*. (2020) studied the stability of rectangular tunnels under surcharge loading in cohesive-frictional soils. Abbo *et al*. (2013) and Wilson *et al*. (2017) studied the stability of rectangular tunnels in cohesive soils. Yang and Qin (2014) carried out limit analysis on rectangular openings under seepage forces. Dutta and Bhattacharya (2019) studied the stability of rectangular tunnels in cohesionless soils.

All the studies mentioned above are for circular, square, and rectangular tunnels in soils without any admixture treatment. However, tunnelling in soft clayey soil conditions without any ground improvement may lead to excessive ground deformations and collapse. In the last few decades, jet grouting (*JG*) and deep cement mixing (*DCM*) ground improvement techniques have been utilized to perform cement-stabilization around the tunnel boundary; the function is to prevent the large deformations and failure, or to control seepage (e.g., Arroyo *et al.* 2011, Croce *et al*. 2014). Table 2 summarises the details of some of the tunnelling projects from worldwide, in which cement-treatment was performed to improve the surrounding soil.

Tyagi *et al.* (2017) studied the failure behaviour of large single tunnel of 12 m diameter excavated in cement-treated soil, using centrifuge and numerical modelling. They named the region of cement-treatment as the 'improved soil surround'. Tyagi *et al.* (2017) observed three failure modes, (a) 'shear' failure in weak and thin improved soil surrounds, (b) 'rupture' failure in intermediate strength improved soil surrounds, (c) 'tension' failure in higher strength and thicker improved soil surrounds. A failure chart and modified stability equation for single circular tunnel was also proposed by Tyagi *et al*. (2017). Tyagi *et al*. (2018, 2020), Pan *et al.* (2020) further studied the effect of spatial variability in cement-treated soils on the stability of large diameter circular tunnels. Recently, Tyagi and Lee (2022)

*Corresponding author, Assistant Professor
E-mail: akanksha.tyagi@ce.iitr.ac.in
[a]M.Tech. Student
E-mail: siddharth_p@ce.iitr.ac.in

ISSN: 2005-307X (Print), 2092-6219 (Online)

studied the effect of nearby tunnel failure on the large diameter tunnel in soil improved by cement-treatment. Zulkefli *et al*. (2017) conducted the centrifuge model tests at 100g to study the failure behaviour of large rectangular tunnel of width, *B* and height, *H* of 30 m and 8 m, respectively with improved soil surround in soft kaolin clay. Four model tests were conducted with unconfined compressive strength of improved soil surround, q_{ui} of 576, 600, 1352 and 1200 kPa, respectively. The thickness of the improved soil surround, *t* was kept as 3 m and 5 m. The depth of cover, *C* was kept as approximately 18 m. Zulkefli *et al*. (2017) measured the variations of the stress at the roof of the tunnel and tunnel support pressure at the springline to compute the critical tunnel support pressure termed TSP_c, at the initiation of failure. Similar to Tyagi *et al.'s* (2017) findings, the value of TSP_c decreased with the increase in strength and thickness of improved soil surround. Therefore, there are experimental as well as numerical studies available for circular tunnels in soils improved by cement-treatment. However, numerical studies and design guidelines for non-circular geometry are limited.

In this paper, the stability and failure behaviour of wide rectangular tunnel in improved soil surround is studied using finite element modelling. The concept of improved soil surround as temporary support provided for the excavation of a rectangular opening is shown in Fig. 1. The function of improved soil surround is to prevent the collapse during tunnel construction and also reduce deformations and disturbance to nearby structures caused due to tunnelling. In a practical scenario, the subsequent lining can be provided after excavation, e.g., construction of the Davidson tunnel and Undercrossing tunnel at San Francisco (Pellegrino and Adams, 1996), KVMRT TU8 tunnel drive, Malaysia, (Raju *et al*. 2021). However, the installation of lining shall not be discussed in this paper.

In the present study, the plane strain finite element model is first developed in a geotechnical finite element software Plaxis 2D. The numerical model is validated with the results of centrifuge model tests performed by Zulkefli *et al*. (2017). The failure behaviour and stability characteristics of rectangular tunnel with improved soil surround are studied for different strength and thickness of improved soil surround, and cover depths. Based on the parametric studies, a failure chart is developed for rectangular tunnels with improved soil surrounds with different strengths, thicknesses, and cover ratios. Finally, a modified stability equation, and a stability chart for rectangular tunnel in improved soil surrounds are proposed which may serve as preliminary design guidelines for constructing such tunnels.

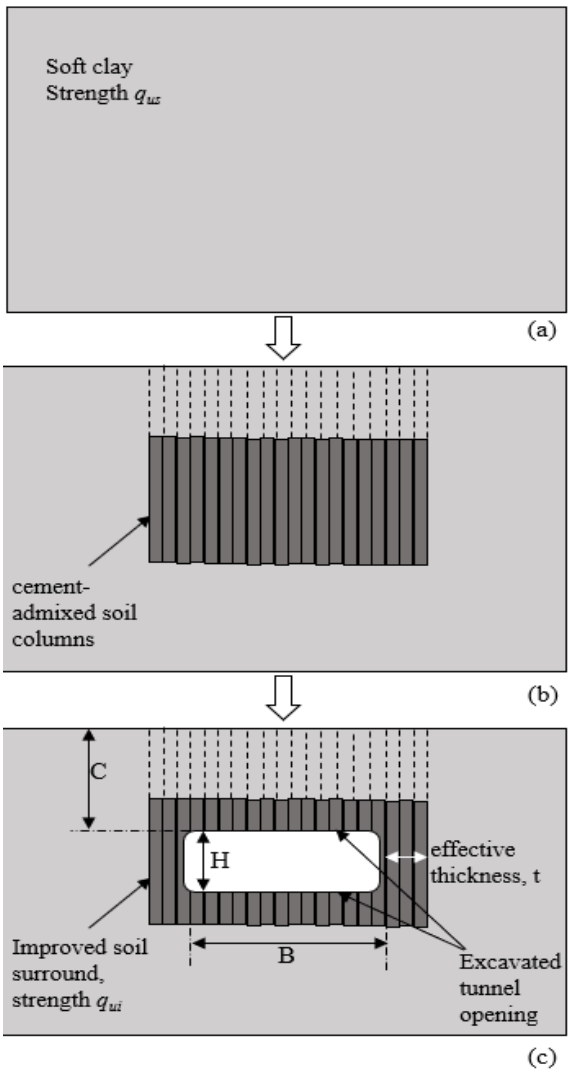

Fig. 1 Schematics showing concept of improved soil surround as temporary support for the excavation of a rectangular opening (a) soft clays without any treatment, (b) cement-admixed soil columns installed using ground improvement technique (deep cement mixing or jet grouting) to provide temporary support for future excavation and (c) excavation done to create rectangular tunnel opening

2. Numerical model

2.1 Geometry and materials

The plane strain finite element model for rectangular tunnel with improved soil surround is shown in Fig. 2. The tunnel geometry and cover depth are kept similar as those of Zulkefli *et al.*'s (2017) centrifuge model test set up. The width and height of the improved soil surround are kept as 30 m and 8 m, respectively. Only half of the geometry is modelled taking advantage of the symmetry. The right-side boundary is taken as 2 times the tunnel width from the centreline of the tunnel. Preliminary boundary studies showed that extending the side boundary to *3B* had no influence on the numerical results. The bottom boundary is kept at 30 m from the tunnel floor, similar to the Zulkefli *et al.* (2017) centrifuge test model.

The cover *C* is kept as 18 m. The equivalent diameter of tunnel opening, D_{eq} is computed as 17.5 m approx. from the following relationship

$$D_{eq} = \sqrt{\frac{4(H \times B)}{\pi}} \quad (1)$$

Table 1 Some examples of non-circular tunnels constructed in recent years across the globe

S no.	Tunnel name/ Location	Type of Surrounding Soil	Surrounding Soil strength	Shape	Geometry	Cover Depth, C	C/D or C/D_{eq}	Reference
1	Shanghai (China)	-	c=0 ϕ=30º	Sub Rectangular	B=9.7 m H= 7.2 m D_{eq}= 9.76	20 m	2.0	Pham *et al.* (2021)
2	Pedestrian Under Pass, Xian (China)	Saturated Loess	-	Rectangular	B=3 m H=9 m D_{eq}=9.42 m	7.4 m	1.26	Wang *et al.* (2018)
3	Fujiayao Tunnel Zhonghe (China)	Alluvial loess	c=22 kPa ϕ =28º	Horse Shoe	B=17 m H=11 m D_{eq}=15.4 m	112 m	8.2	Qiu *et al.* (2018)
4	Kil Tunnel (Netherland)	-	-	Rectangular	B=31 m H=8.75 m Deq=18.5 m	--	--	Gavin *et al.* (2019)
6	Suzhou (China)	Silty Sand	c=3.8 kPa ϕ=33.4º	Rectangular	B=9.1 m H=5.5 m D_{eq}=8.0 m	9m	1.3	Chen *et al.* (2019)
8	Fréjus road tunnel (France)	Lustorous schist	UCS vary between 30 MPa and 100 MPa	Horse shoe shaped tunnel	B=11.6 m	Over 1000 m	--	Fuente *et al.* (2019)
10	Suzhou Tunnel (China)	Silty Clay and Silty Sand	c=23.4 kPa, ϕ=12.9º (Silty Clay) c=5.2 kPa, ϕ=31.1º (Silty Clay)	Rectangular	B=6.9 m H=4.2 m D_{eq}= 6.1 m	4..1	0.76	Liu *et al.* (2021)
11	Kumming Under Pass (China)	Silty Clay and Fine Sand	-	Rectangular	B=6.9 m H=4.9 m D_{eq}=6.56 m	4.5 m	0.77	Wang *et al.* (2020)

*D_{eq} is calculated from Eq. (1)

Table 2 Strength and geometry parameters for tunnelling projects in improved soil surround

Project Name	Surrounding soil	Diameter, *D* (Excavation limit) (m)	*C/D* ratio	Minimum strength requirement for improved soil, q_{ul} (kPa)	Minimum thickness-to-diameter ratio, *t/D*	Reference
Dhauby Ghaut MRT (Singapore)	Soft marine clay	6.6	--	300	0.23	Tornaghi and Cippo (1985)
Robinson road tunnels (Singapore)	Soft marine clay	6	~1.8 & ~3	--	0.25	Ganeshan and Yng (2009)
Milan Subway (Italy)	Mixtures of sands and gravel, silt	8.7	~1 to ~1.5	--	--	Contini *et al.* (2007)
Davidson Tunnel (San Francisco Bay)	Bay mud-soft NC/ slightly OC clays	4.6	-	830	0.26	Pellegrino and Adams (1996)
Undercrossing Tunnel (San Francisco Bay)		4.1	~3.5	830	0.29	
Klang Valley MRT (Malaysia)	Sandy silt, layers of soft clay	~6.5	~0.9 to ~1.4	1500	Depth of improvement is from surface to rock level	Yee and Tan (2015)

Thus, the cover ratio *CR*, defined as the ratio of cover to equivalent diameter of tunnel opening, may be taken as approx. 1.0 for the validation model. The thickness ratio *TR* is defined as the ratio of thickness of the improved soil surround to equivalent diameter.

The side boundaries are constrained in horizontal direction, while the bottom boundaries are fixed in both horizontal and vertical directions. The 15-noded plane strain triangular element are adopted for the analysis and total 7632 elements, 15413 nodes are generated after meshing.

The mesh is kept fine within improved soil surround and the region surrounding it. The maximum element size for improved soil surround is adopted as approximately 0.25 m, while coarser mesh with maximum element size is adopted near the boundaries (see Fig. 2(b)).

Two materials are present in the model, the untreated soft clay and the cement-treated soft clay. The untreated clay is modelled using Modified Cam Clay, and the input properties are shown in Table 3. Following Tyagi *et al.* (2017, 2020), the cement-treated soft clay is modelled as Mohr-Coulomb material with effective strength and stiffness parameters (c', ϕ, E', v'). The effective cohesion c' and angle of friction ϕ' are related to the unconfined compressive strength q_{ui} by

$$c' = \left(\frac{q_{ui}/2}{\sin \phi'} - q_{ui}/2 \right) \tan \phi' \quad (2)$$

As discussed in Tyagi *et al.* (2017), the reason is that the coefficient of consolidation for cement-treated clays is as high as 50 times to that of the natural clays, (Terashi and Tanaka 1983, Terashi *et al.* 1980). Tyagi and Lee (2017) have shown for cement-treated clays, that the dimensionless time of approximately ≥ 1 is computed for a standard strain-rate of 1 mm/min, indicating nearly drained situation in unconfined compression test. Past researchers e.g., Chin

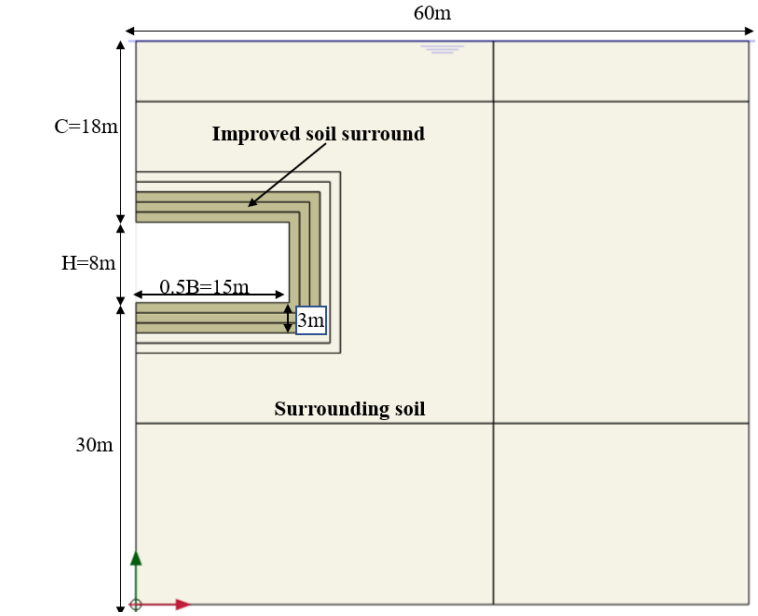

(a)

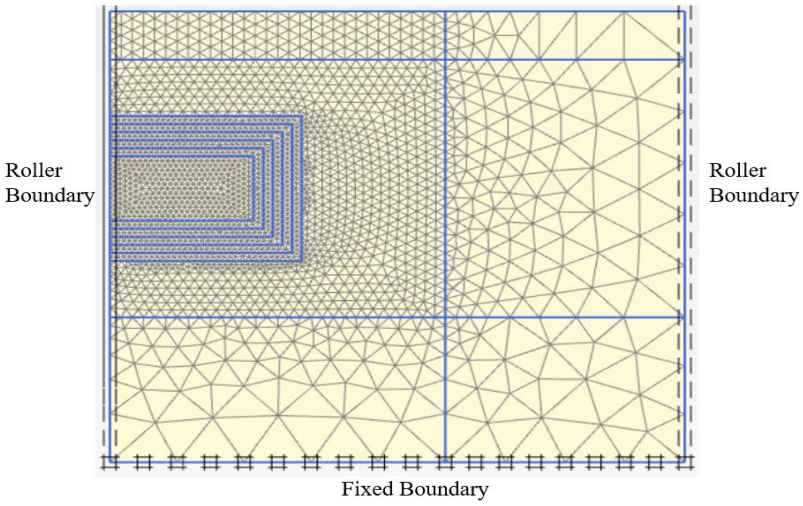

(b)

Fig. 2 Plane strain finite element model (a) showing geometry and materials (b) mesh and boundary conditions

(2006), Xiao (2009), Tyagi *et al.* (2019) have also observed water droplets from the cement-treated soil samples during unconfined compression tests. This is another indication of drainage during testing.

In addition to Mohr-Coulomb model with effective properties, the tension-cut off is also modelled with the tensile strength kept as 13% of q_{ui} (Pan *et al*. 2016, Xiao 2009, Tyagi *et al*. 2017) and is graphically shown in Fig. 3. Non-associated flow rule with zero angle of dilation is used in the Mohr-Coulomb model for modelling cement-treated soil, and hence, no volume change is expected during post-yielding for the cement-treated soil. The properties of the cement-treated clay are summarized in Table 3.

2.2 Modelling tunnel excavation

As shown in Fig. 4(a), the modelling starts with the 'Initial' step in which only soft clay bed was modelled. It is followed by the 'Replacement' step in which the zone of soft soil is removed with the improved soil, Fig. 4(b). Note that the installation effects of the improved columns have not been the focus of this research. Any minor deformations that took place in replacement step were brought to null value at the start of the next step. As shown in Fig. 4(c), the replacement step is then followed by the 'Apply Pressure step' in which the soil is replaced with the full support pressure applied at the crown, along the side, and invert of the tunnel. To find the critical tunnel support pressure (TSP_c), the support pressure is then reduced at a slow rate of 1% in each subsequent step till analysis is terminated due to excessive plastic points and soil deformation.

The excavation procedure herein replicates the centrifuge test procedure in which the excavation was carried out by releasing the fluid pressure inside the tunnel (Zulkefli *et al*. 2017). Similar excavation procedures in soft clays were also adopted by early researchers, e.g., Mair

Table 3 Properties of natural and cement-treated clay

Material	Geotechnical Properties	Values	References
Natural Clay (Modified Cam Clay)	Isotropic Swelling Index, κ	0.054	Li (2014) *, Tyagi *et al*. (2017)
	Isotropic Compression Index, λ	0.23	
	Critical state friction coefficient, M	0.9	
	Unit weight (kN/m^3)	16	
	Over consolidation ratio	1	
	Strength, q_{us} (kPa)	$0.28\sigma_v'$	
Cement-treated clay (Mohr Coulomb Undrained A)	Effective Modulus, E' (kPa)	160 q_{ui}	Tan *et al*. (2002), Tyagi *et al.* (2017)
	Effective cohesion, c' (kPa)	0.23 q_{ui}	Tyagi *et al.* (2017)
	Unit weight (kN/m^3)	16	Tyagi *et al.* (2017)
	Angle of friction, ϕ' (degrees)	41	Broms (2004), Xiao (2009)
	Poisson's ratio, υ'	0.2	Kitazume and Terashi (2013)
	Tensile strength, σ_t (kPa)	0.13 q_{ui}	Pan *et al*. (2016), Xiao (2009), Tyagi *et al.* (2017)

*After Y.P. Li, personal communication (2014)

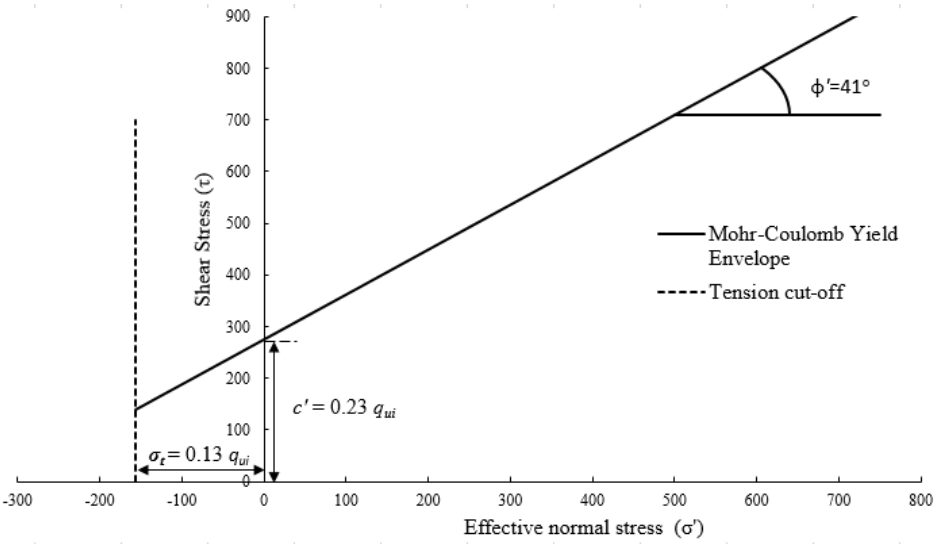

Fig. 3 Mohr-Coulomb model with effective strength properties and tension cut-off to model cement-treated clay

(1979), Casarin and Mair (1981). In tunnelling operations through soft clays, the unlined heading is supported by the pressurized slurry. This temporary support is required to prevent failure and undesirable deformations. Hence, the aforementioned procedure allows for determining the magnitude of the temporary support pressure required for a stable improved soil surround. Moreover, the objective of this study is not to model a specific construction procedure, but to model an idealised tunnel excavation that would be assumed by the designer.

3. Validation of numerical model with Zulkefli *et al.* (2017) centrifuge result

3.1 Failure modes and critical tunnel support pressure

Zulkefli *et al.* (2017) conducted four model tests with q_{ui} of 576 kPa, 600 kPa, 1352 kPa, and 1200 kPa, respectively, and thickness of 3 m and 5m.

The details of the corresponding numerical models that are developed in the present study are summarized in Table 4.

Tyagi *et al.* (2017) and Zulkefli *et al.* (2017) both defined the TSP_c as the magnitude of tunnel support pressure at which the failure initiates in the improved soil surround. Tyagi *et al.* (2017) observed low magnitude of displacements for improved soil surround in centrifuge tests, and hence stresses were monitored at the crown and springline to measure TSP_c in the physical model tests. Tyagi *et al*. (2017) also performed numerical modelling and stress states, instead of displacement, were used to define the failure criteria. Zulkefli *et al*. (2017) also monitored stress at the crown to obtain the TSP_c for the rectangular improved soil surround in centrifuge model tests.

Following Tyagi *et al*.'s (2017) study, the TSP_c in the present numerical study is defined when one of the

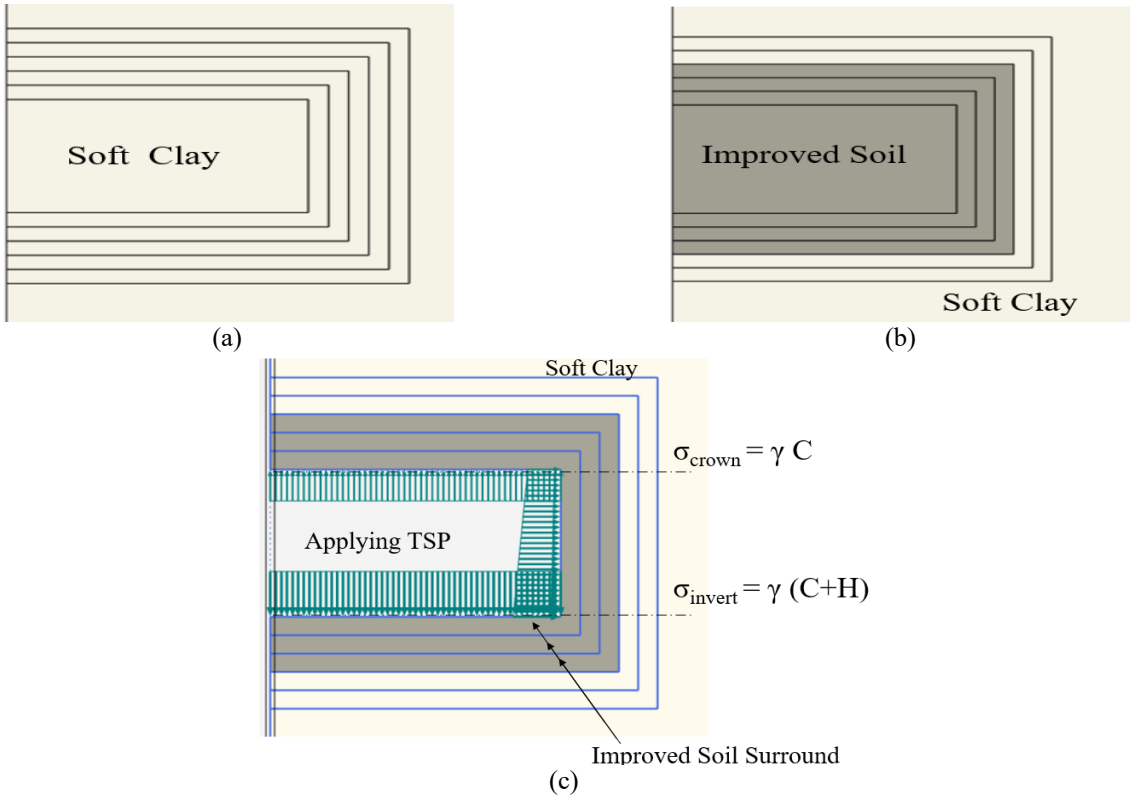

Fig. 4 Steps for modelling excavation (a) Initial Step (b) Replacing soft soil with improved soil (c) Removal of improved soil elements and applying tunnel support pressure inside tunnel periphery

following failure modes occurs:

- Shear failure – when yielding occurs across the thickness of improved soil surround,
- Tension failure - when tension points occur (to at least 1 m thickness) in the improved soil surround,
- Rupture failure – when shearing and tension co-occur.

The stress states for the *NT3_576* along with the values of tunnel support pressures as observed numerically, are shown from Figs. 5(a)-5(d). As the tunnel support pressure is reduced, the plastic points start to develop at the inner corner and tunnel roof, while tension points start to develop at the outer corner of improved soil surround, Fig. 5(a). As the excavation progressed, the yielding increases from the inner corner to the outer corner of the improved soil surround, indicating the primary failure mode as 'shear failure', Fig. 5(b). The shear failure is usually accompanied by roof collapse and large deformations. Zulkefli *et al.* (2017) also observed multiple cracks along with roof collapse with large deformations for the corresponding centrifuge test, (for picture, refer Zulkefli *et al*. 2017).

For *NT5_600*, the yielding starts from the inner corner of the tunnel similar to lower thickness improved soil surround *NT3_576*, as shown in Fig. 6(a). However, for 5 m thick tunnel, the tension failure is observed at the centreline near the periphery of the improved soil surround, Fig. 6(b). Therefore, for *NT5_600* the primary failure mode is defined as the 'tension failure'. As shown in Fig. 6 (c), as the tunnel support pressure reduced, the tension and shear occur simultaneously at the corner of the tunnel, leading to rupture failure at that location. Zulkefli *et al.* (2017) also observed tension and rupture cracks at the centre of roof and at the corners of the improved soil surround (for pictures, refer Zulkefli *et al.* 2017).

Table 4 Details of numerical models for validation

S.No.	Model ID	Strength of improved soil surround, q_{ui} (kPa)	Thickness of improved soil surround, t (m)	t/D_{eq}	C/D_{eq}
1	NT3_576	576	3	0.17	1.0
2	NT5_600	600	5	0.29	1.0
3	NT3_1352	1352	3	0.17	1.0
4	NT5_1208	1208	5	0.29	1.0

As shown in Figs. 7(a)-7(d), for *NT3_1352*, as the tunnel support pressure is reduced, the tension points appear at the inner and outer roof as well as the corners of improved soil surround, indicating tension failure at those locations. This is also in agreement with the observations of Zulkefli *et al*. (2017). Similarly, tensile failure mode is observed as the dominant failure mode for *NT5_1208,* which had stronger and thicker improved soil surround.

Table 5 summarises the values of critical tunnel support pressure for the four test models. It can be observed that the values of TSP_c obtained numerically are in good agreement with the Zulkefli *et al*. (2017) centrifuge test results.

3.2 Crown deformation and critical tunnel support pressure

As an alternate approach, the TSP_c are also obtained

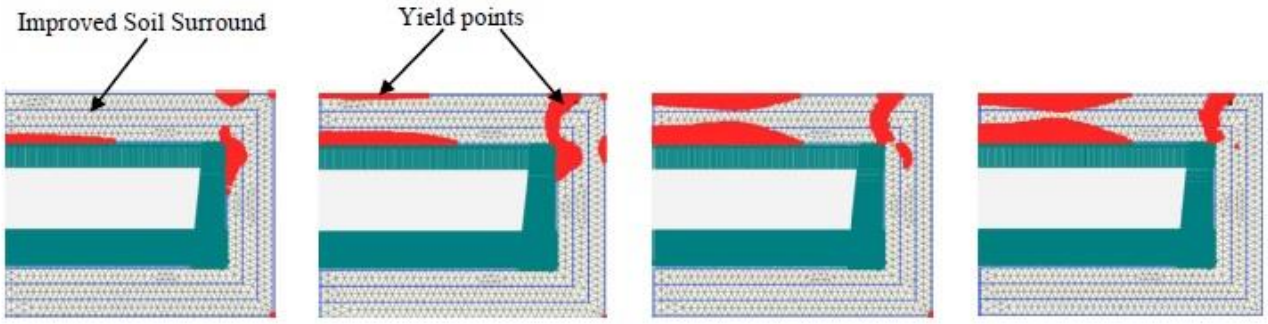

(a) (b) (c) (d)

Fig. 5 Failure modes for *NT3_576* at tunnel support pressure (a) 327.4 kPa, (b) 323.8 kPa, (c) 320.3 kPa and (d) 316.8 kPa

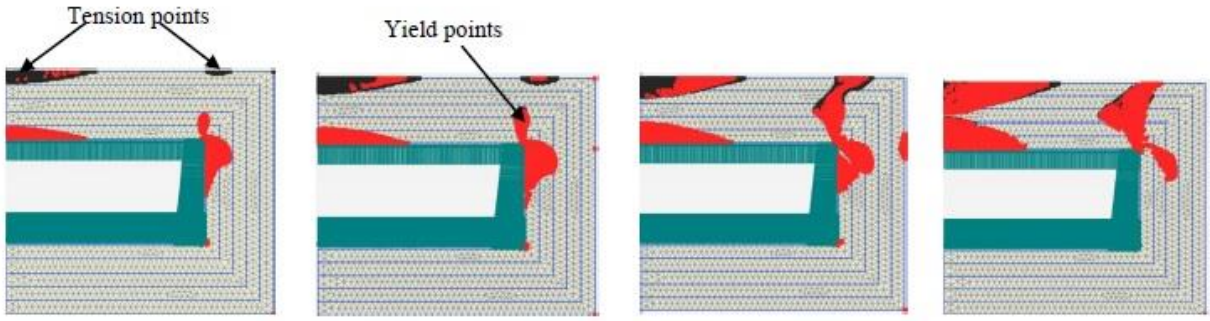

(a) (b) (c) (d)

Fig. 6 Failure modes for *NT5_600* thickness at tunnel support pressure (a) 313.3 kPa, (b) 309.8kPa, (c) 306.2 kPa and (d) 302.7 kPa

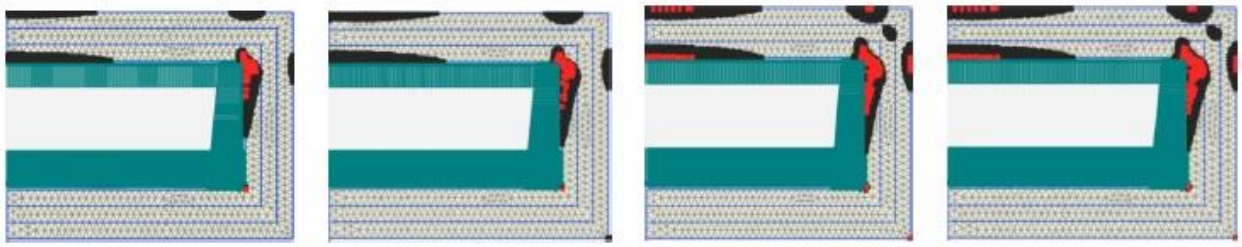

(a) (b) (c) (d)

Fig. 7 Failure modes for *NT3_1352* at tunnel support pressure (a) 320.3 kPa, (b) 316.8 kPa, (c) 313.3 kPa and (d) 309.8 kPa

Table 5 Results of numerical model and comparison with centrifuge tests results

S.No.	Model ID	TSP_c from Zulkefli *et al.* (2017)	*TSPc* from numerical (Failure mode criteria)	Difference from Zulkefli *et al.* (2017)	Primary Failure mode	TSP_c from numerical (displacement criteria)	Difference from Zulkefli *et al.* (2017)
		(kPa)	(kPa)	(%)		(kPa)	(%)
1	NT3_576	337	323.8	3.9	Shear	324.5	3.7
2	NT5_600	323	309.8	4	Tension	307.2	4.89
3	NT3_1352	328	316.8	3.4	Tension	308.5	5.9
4	NT5_1208	321	309.8	3.4	Tension	285.5	11

from the crown deformation by taking the tangents for the elastic and plastic portion of the displacement plots, Figs. 8 and 9. High crown deformations are observed for lower thickness and strength improved soil surround *NT3_576*, in which shear failure was dominant failure mode. Less crown deformations are observed for thicker improved soil surrounds, i.e., *NT5_600* and *NT5_1208*. As shown in Table 5, except for *NT3_576* which is weak and thin tunnel, the

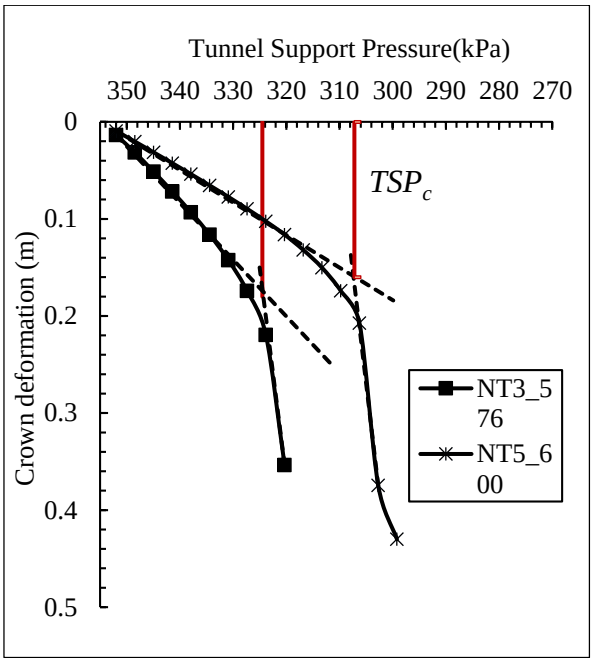

Fig. 8 Tunnel crown deformation plotted against tunnel support pressure for *NT3_576* and *NT5_600*

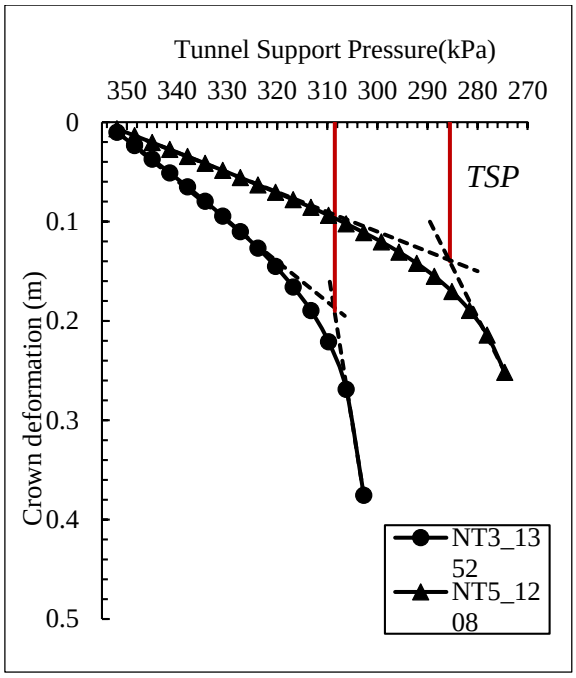

Fig. 9 Tunnel crown deformation plotted against tunnel support pressure for *NT3_1352* and *NT5_1208*

TSP_c obtained from the failure modes criteria are mostly higher than the TSP_c obtained from the displacement criteria. This further strengthens the hypothesis that the stress states are better indication of the incipient failure than the displacements for such improved soil surrounds.

3.3 Effect of rounded corners

The geometry adopted by the Zulkefli *et al.* (2017) and the numerical model discussed in previous section have

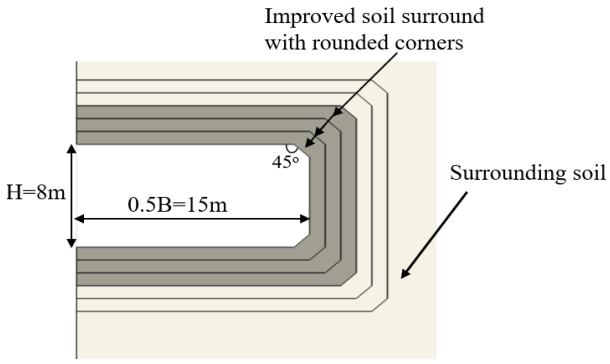

Fig. 10 Rectangle geometry with rounded corners

rectangular tunnel with sharp corners that has the limitation of stress-concentration at the corners. The maximum compressive stresses are always concentrated near the corners that increase the probability of failure at the corners (Zhoa *et al*. 2021). Caudle and Clark (1955) also mentioned that to reduce the stress concentration in rectangular openings, the opening should be provided with rounded corners. For actual tunnels, the rectangular openings with sharp corners are less preferred, instead the rounded corners such as shown in Fig. 1(c) are more common

Thus, the four test models are again compared with rounded corner geometry (see Fig. 10). All other parameters and properties are kept same as in the validation model.

Table 6 compares the TSP_c values obtained for the two numerical models, i.e., one with sharp corners and the other with rounded corners. It can be observed that except for the *NT3_576*, the results for the other three test models are same. This may be due to the fact that the *NT3_576* is characterized by a thin and weak tunnel of less thickness and lower strength and thus, the effect of sharp corners is more profound in the weaker improved soil surrounds. Since, the rectangular tunnel with rounded corner geometry is more common in the practical scenario, the same numerical model is adopted for all the parametric studies in this paper.

4. Parametric studies

4.1 Details of parameters

In this study, the values of strength, and thickness of the rectangular improved soil surround and the cover are varied. As Table 7 shows, the strengths are varied from 200 kPa to 4000 kPa, thickness ratios are varied from 0.06 to 0.29 and cover ratios are varied from 1.0 to 2.7. The adopted range is in agreement with the design values for actual ground improvement projects presented in Table 2. Recently, Tyagi and Tamta (2023) reported mean strengths for cement-treated clays in the range of 2.1 to 10.6 MPa for *DCM* and *JG* sites. In the present study, the strengths are further categorised as low strength i.e., $200 \leq q_{ui} < 600$ kPa, intermediate strength i.e., $600 \leq q_{ui} < 2000$ kPa, and high strength i.e., $2000 \leq q_{ui} \leq 4000$ kPa. Based on thickness ratios, the tunnels are also classified as thin, thick, and having intermediate thickness, i.e., $0.06 \leq TR < 0.11$ as thin,

Table 6 Comparison of results of numerical model with rectangular geometry having sharp corners and rounded corners with centrifuge test results

S.No.	Name ID	TSP_c from Zulkefli *et al.* (2017)	TSP_c from numerical (Failure mode criteria) Rectangle with sharp corners	Difference from Zulkefli *et al.* (2017)	TSP_c from numerical (Failure mode criteria) Rectangle with rounded corners	% difference from Zulkefli *et al.* (2017)
		(kPa)	(kPa)	(%)	(kPa)	(%)
1	NT3_576	337	323.8	3.9	316.8	5.9
2	NT5_600	323	309.8	4	309.8	4
3	NT3_1352	328	316.8	3.4	316.8	3.4
4	NT5_1208	321	309.8	3.4	309.8	3.4

(a) (b) (c)

Fig. 11 Failure modes for improved soil surround with TR = 0.17, CR =1.0 (a) Shear Failure, q_{ui} = 200 kPa, $NTSP_c$ = 93%, (b) Rupture Failure, q_{ui} = 600 kPa, $NTSP_c$ = 90% and (c) Tension Failure, q_{ui} = 2500 kPa, $NTSP_c$ = 86%

(a) (b) (c)

Fig. 12 Failure modes for improved soil surround with q_{ui} = 600 kPa, CR =1.0; (a) Shear Failure, TR = 0.06, $NTSP_c$ = 94%, (b) Rupture Failure, TR = 0.17, $NTSP_c$ = 90% and (c) Tension Failure, TR = 0.29, $NTSP_c$ = 88%

Table 7 Values adopted for parametric study

Parameter	Values
q_{ui} (kPa)	200, 400, 600, 800, 1000, 1200 1500,2000, 2500, 3000, 4000
t (m)	1, 2, 3, 4, 5
TR (t/D_{eq})	0.06, 0.11, 0.17, 0.23, 0.29
C (m)	18, 31, 46.5
CR (C/D_{eq})	1.0, 1.8, 2.7

$0.11 \leq TR < 0.23$ as intermediate thickness, and $TR \geq 0.23$ as thick improved soil surround

4.2 Effect of strength and thickness

The parametric study is conducted by varying the strength and thickness of improved soil surround for a CR of 1.0. The normalised tunnel support pressure ($NTSP_c$) is defined as the ratio of the critical tunnel support pressure to the full tunnel support pressure computed at the springline, just prior to the start of excavation.

Fig. 11 shows the observed failure modes for different strengths with the same TR and CR. It is observed that for the low strength, shear failure is primary failure mode; for intermediate strength, rupture failure is the primary failure mode, while for higher strength, tension failure is dominant. The observations are in good agreement with Tyagi *et al.* (2017) observations for large diameter circular tunnel in clays improved by cement-treatment.

Fig. 12 shows the observed failure modes for different TR of improved soil surround with the same q_{ui} and CR. It is observed that for intermediate strength, thin improved soil surround, the shear failure is primary failure mode; for intermediate thickness, rupture failure is the primary failure mode, while for thick improved soil surround, tension failure is dominant.

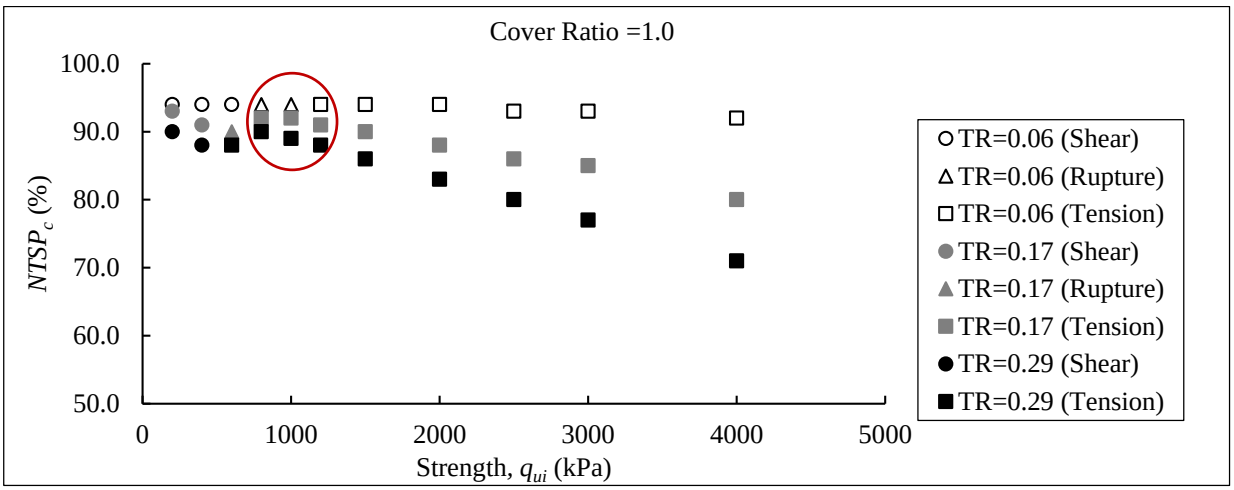

Fig. 13 Plot of Normalised Tunnel support pressure ($NTSP_c$) vs strength of improved soil surround marked circle represents the transition cases from shear to tension failure mode

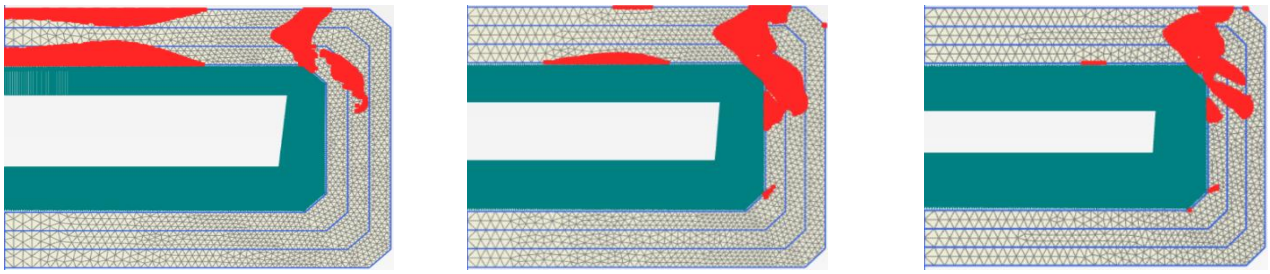

(a) (b) (c)

Fig. 14 Failure modes observed for improved soil surround, q_{ui} = 400 kPa, TR = 0.17; (a) CR =1.0, q_{ui}/q_{us} = 5.4, $NTSP_C$ = 91%, (b) CR = 1.8, q_{ui}/q_{us} = 3.4, $NTSP_C$ = 88% and (c) CR = 2.7, q_{ui}/q_{us} = 2.4, $NTSP_C$ = 85%.

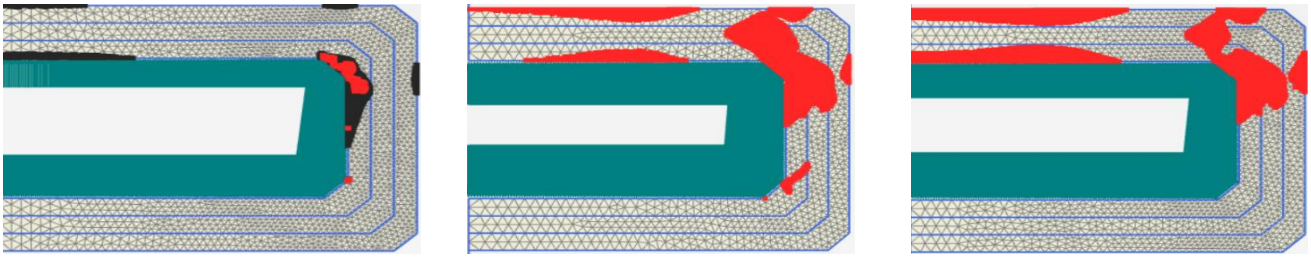

(a) (b) (c)

Fig. 15 Failure modes of tunnel at q_{ui} = 1000 kPa, TR = 0.17 (a) CR=1.0, q_{ui}/q_{us} = 13.5, $NTSP_C$= 92%, (b) CR=1.8, q_{ui}/q_{us} = 8.5, $NTSP_C$ = 85% and (c) CR = 2.7, q_{ui}/q_{us} = 5.9, $NTSP_C$ = 82%.

As shown in Fig. 13, the critical tunnel support pressure decreases with the increase in the strength as well as thickness of improved soil surround. There are few exceptions to this trend which occurred at the transitional failure modes. Nevertheless, the general finding suggests that the stability of rectangular tunnel in cement treated improved soil surround increases with the increase in both thickness and strength of improved soil surround.

4.3 Effect of cover

The failure modes were observed to be different for the low, intermediate, and high strength improved soil surrounds, therefore, the effect of cover is studied for each failure mode separately.

First, the effect of cover is studied for the low strength improved soil surround with q_{ui} = 400 kPa. As shown in Figs. 14(a)-14(c), the improved soil surround showed shear failure for all three cover ratios i.e., CR =1.0, 1.8 and 2.7 with the reduction in values of $NTSP_c$ from 91%, 88% to 85%, respectively. This indicates that the stability increases with the cover depth for the tunnels with weaker improved soil surround. This trend is same as demonstrated by the tunnels in soft soils without any improvement, (e.g., Casarin and Mair 1981, Kimura and Mair 1981). The reason is attributed to the smaller magnitude of the difference between the stresses acting at the crown and invert of the tunnel for deeper tunnels as compared to the original in situ overburden stresses.

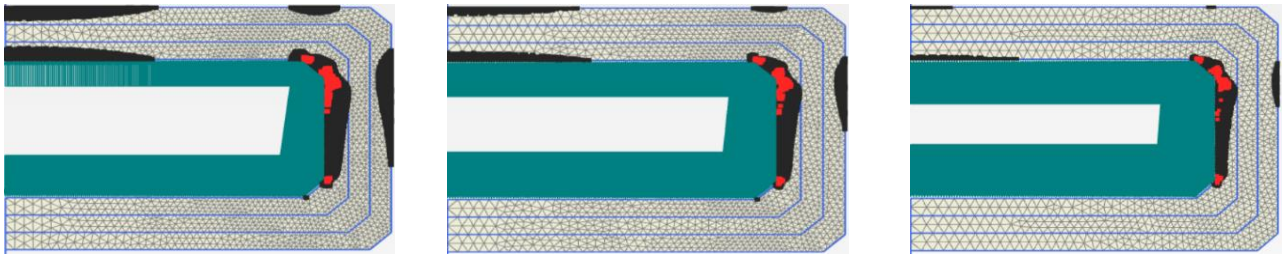

(a) (b) (c)

Fig. 16 Failure modes of tunnel at q_{ui} = 4000 kPa, TR = 0.17 (a) CR=1.0, q_{ui}/q_{us} = 54.1, $NTSP_C$= 80%, (b) CR=1.8, q_{ui}/q_{us} = 34.0, $NTSP_C$= 84% and (c) CR=2.7, q_{ui}/q_{us} = 23.6, $NTSP_C$= 85%

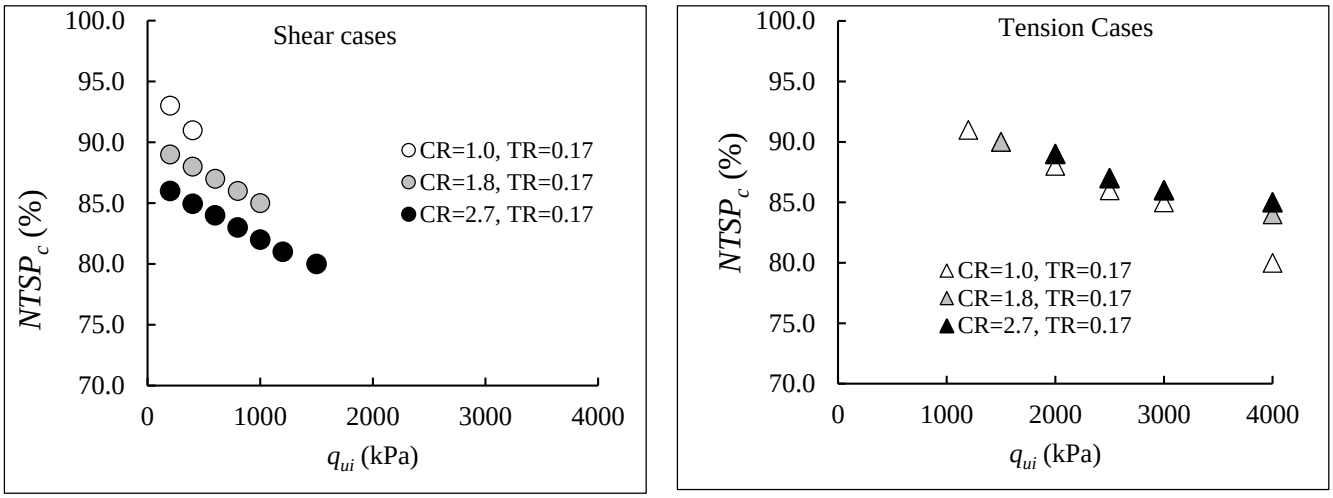

(a) (b)

Fig. 17 Normalised critical tunnel support pressures plotted against strength of improved soil surround for different cover ratios (a) Shear cases and (b) Tension cases

Similar behaviour is portrayed by the improved soil surround with intermediate strength q_{ui} = 1000 kPa, in which the values of $NTSP_c$ decreased with the increase in cover depth. As shown in Figs. 15 (a)-15(c), as the cover depth increases, the dominant failure mode also transitions from tension failure to shear failure. The results indicate that the failure behaviour is related to the ratio of the strength of improved soil surround to the strength of surrounding soil i.e., q_{ui}/q_{us}, rather than just q_{ui}.

The effect of cover depth is also studied for the stronger improved soil surround with q_{ui} = 4000 kPa. Figs. 16(a)-16(c) show the contrasting behaviour, in which the values of $NTSP_c$ increased with the increase in cover depth, indicating decrease in stability. This may be attributed to the fact that for strong tunnels, the strength of the surrounding soil is very small as compared to the strength of the improved soil surround, i.e., $q_{us} << q_{ui}$. Hence, the original stress state of in situ soil does not play a significant role in stability and the surrounding soil acts more like an overburden pressure for the improved soil surround. In this case, as the cover depths increases, the overburden pressure increases on the improved soil surround and hence the stability decreases.

In order to qualify the above discussion, the $NTSP_c$ for shear and tension failure cases are plotted separately in Figs. 17(a) and 17(b). Fig. 17(a) shows lower $NTSP_c$ for higher cover ratios, indicating an increase in the stability for shear cases. On the other hand, Fig. 17(b) shows a little higher $NTSP_c$ for lower cover ratios, indicating a slight decrease in stability. This also suggests that the effect of cover on the magnitude of $NTSP_c$ is less significant for stronger improved soil surrounds.

4.4 Failure chart

The aforementioned discussion indicated that the failure behaviour is more related to the ratio q_{ui}/q_{us}, rather than just the q_{ui}. Keeping in view of the obtained results, failure charts are plotted between the strength ratio and thickness ratio for different cover ratios in Figs. 18(a)-18(c). The figures show that for the rectangular improved soil surrounds, for $q_{ui}/q_{us} < 10$, shear failure is the dominant failure mode, while for $q_{ui}/q_{us} > 10$ and $TR > 0.1$, the tension failure is the dominant failure mode. The rupture failure cases are few and mostly occur for the transition cases between shear and tension failure mode. In Tyagi *et al.* (2017) failure chart for circular improved soil surrounds, the shear failure was dominant for strength ratio $q_{ui}/q_{us} >$ 10 and $0.05<TR<0.15$, while the tension cases were more common for $q_{ui}/q_{us} > 10$ and $TR > 0.15$.

4.5 Stability ratio and chart

Broms and Bennemark (1976) defined the stability ratio

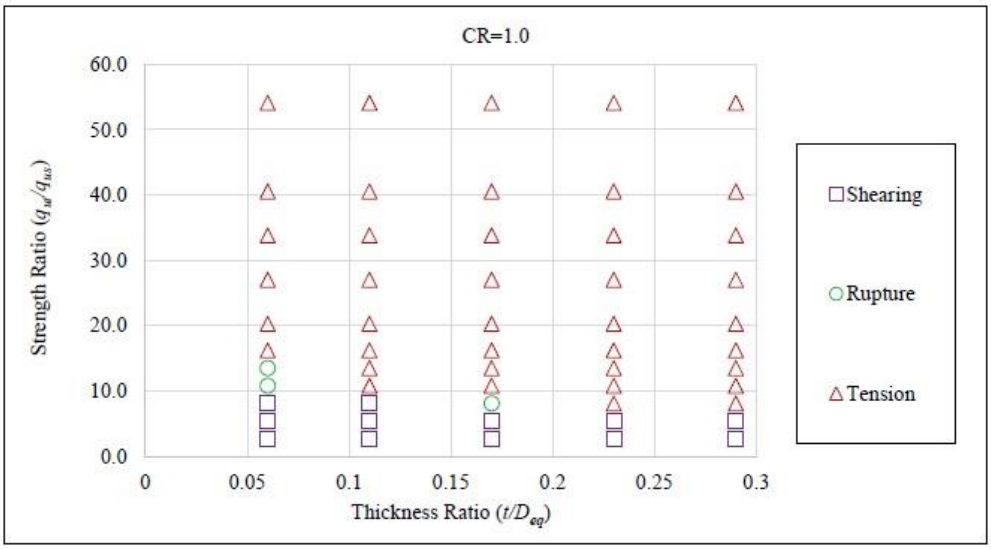

(a)

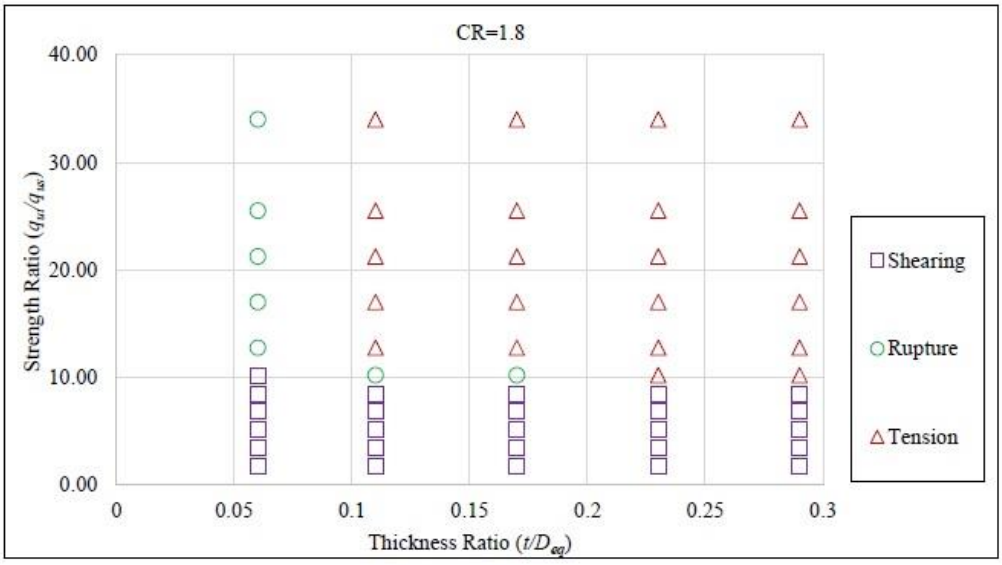

(b)

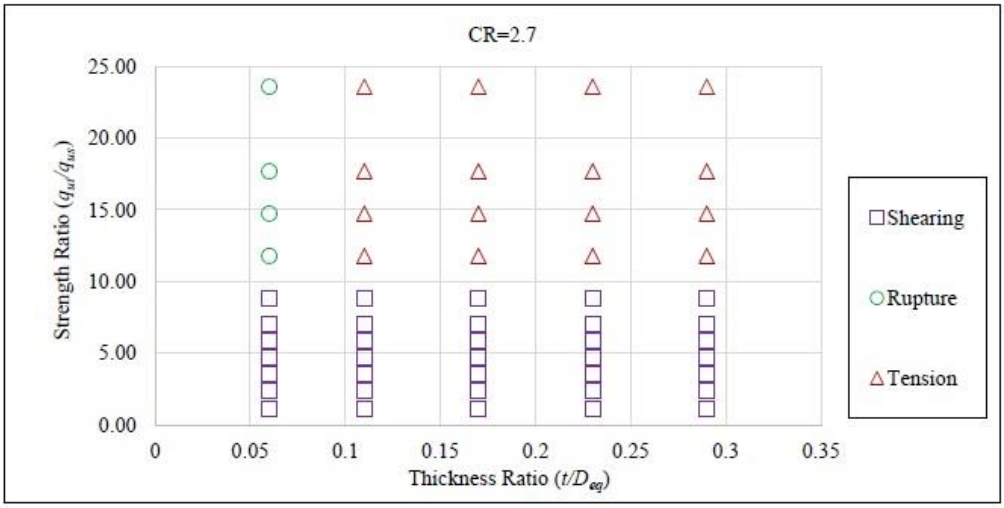

(c)

Fig. 18(a) Failure chart for rectangular tunnels with improved soil surround for *CR* =1.0, (b) Failure chart for rectangular tunnels with improved soil surround for *CR* =1.8 and (c) Failure chart for rectangular tunnels with improved soil surround for *CR* =2.7

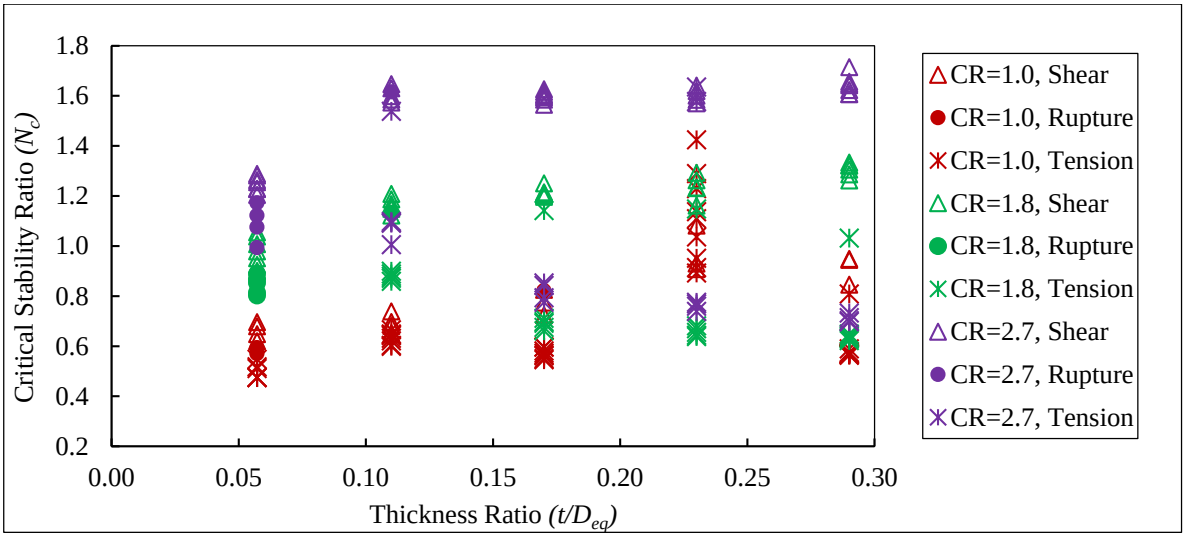

Fig. 19 Proposed stability chart for the rectangular tunnel in improved soil surround.

for untreated clays as the ratio of difference between total overburden stress and the tunnel support pressure at the tunnel springline, to the undrained shear strength. For the circular tunnel in improved soil surrounded by clays, Tyagi *et al*. (2017) defined the stability ratio as

$$N = \frac{\gamma_s\left(C + {}^{D}/_{2}\right) + \sigma_s - \sigma_T}{\left(\alpha_m q_{us}\right) + \left(\beta q_{ui}\, {}^{t}/_{D}\right)} \tag{3}$$

where γ_s is the unit-weight of the natural clay, C is the cover, D is the diameter of tunnel opening, σ_s is the surcharge acting on the ground surface (taken as zero for all cases in this study), σ_T is the tunnel support pressure acting the tunnel springline, t is the thickness of improved soil surround, q_{us} and q_{ui} are the unconfined compressive strengths of the natural clay and treated clay, respectively; α_m is a factor accounting for the difference in the strength mobilization rate of natural clays and treated clays adopted as 0.4, and β is a factor accounting for different types of failure modes, adopted as 0.13.

For a rectangular tunnel, the Eq. (3) may be modified as

$$N = \frac{\gamma_s\left(C + {}^{H}/_{2}\right) + \sigma_s - \sigma_T}{\left(\alpha_m q_{us}\right) + \left(\beta q_{ui}\, {}^{t}/_{D_{eq}}\right)} \tag{4}$$

where H is the height of the rectangular tunnel and D_{eq} is the equivalent diameter of the rectangular tunnel.

Fig. 19 shows the stability chart for critical stability ratio N_c, computed at the critical tunnel support pressure using Eq. (4), for various thickness ratios and cover ratios

5. Conclusions

In this paper, the stability characteristics and failure modes of a wide rectangular opening in improved soil surround were discussed. The influence of strength, and thickness of improved soil surround, and cover depths were studied. For low and intermediate strength tunnels in which 'shear and rupture' were dominant failure mode, the stability was found to increase with the cover. On the other hand, for high strength improved soil surround with 'tension' as the dominant failure mode, the stability was found to decrease with the cover. The reason for such contrasting behaviour is that for strong tunnels, the strength of the natural clay is marginal as compared to the strength of the improved soil surround. Hence, the surrounding soil acts more like an overburden pressure for the high strength improved soil surround and does not play critical role in stability. In such cases, as the cover depths increases, the overburden pressure increases on the improved soil surround resulting in lower stability. It was also observed that the effect of cover on the magnitude of $NTSP_c$ is less significant for high strength improved soil surrounds.

Results showed that the failure behaviour of tunnel in improved soil surround is dependent on the q_{ui}/q_{us}, rather than just q_{ui}. The failure chart showed that for the rectangular improved soil surrounds, for $q_{ui}/q_{us} < 10$, shear failure is the dominant failure mode, while for $q_{ui}/q_{us} > 10$ and $t/D_{eq} > 0.1$, the tension failure is the dominant failure mode. Few rupture failure cases occur as the transition cases between shear and tension failure mode. The proposed failure chart, modified stability equation, and stability chart can serve as preliminary design guidelines for constructing the rectangular tunnel in clays improved by cement-treatment.

Acknowledgements

The authors would like to thank the Ministry of Education, Govt. of India, for providing financial assistance to the first author during his M.Tech. program.

References

Abbo, A.J., Wilson, D.W., Sloan, S.W. and Lyamin, A.V. (2013), "Undrained stability of wide rectangular tunnel", *J. Comput.*

Geotech., **53**, 46-59**.** https://dx.doi.org/10.1016/j.compgeo.2013.04.005.

Arroyo, M., Gens, A., Croce, P. and Modoni, A. (2011), "Design of jet-grouting for tunnel waterproofing", *Proceedings of 7th International Symposium on Geotechnical Aspects of Underground Construction in Soft Ground*, Rome, Italy, May.

Assadi. A. and Sloan, S.W. (1991), "Undrained stability of shallow square tunnel", *J. Geotech. Eng.*, **117**(8), 1152-1173. https://doi.org/10.1061/(ASCE)0733-9410(1991)117:8(1152)

Broms, B.B. (2004), "Lime and lime/cement columns", Ground improvement, **2**, (Eds., M.P. Moseley and K. Kirsch), *Taylor & Francis*, London.

Broms, B.B. and Bennemark, H. (1967), "Stability of clay at vertical openings", *J. Soil Mech Found. Division*, **193**(1), 71-94. https://doi.org/10.1061/JSFEAQ.0000946.

Casarin, C. and Mair, R.J. (1981), "The assessment of tunnel stability in clay by model tests", *Soft ground tunnelling, failures and displacements*, (Eds., D. Resendiz and M. Romo), A.A. Balkema, Rotterdam, Netherlands.

Caudle, R.D. and Clark, G.B. (1955), "Stress around mine openings in some geological structures", *University of Illinois Bulletin,* **52**(69), 7-37.

Chen, X., Ma, B., Najafi, M. and Zhang, P. (2019), "Long rectangular box jacketing Project: A Case study", *Undergr. Space*, **6**(2) 101-125. https://doi.org/10.1016/j.undsp.2019.08.003

Chin, K.G. (2006). "Constitutive behaviour of cement treated marine clay", Ph.D. Thesis. National University of Singapore, Singapore.

Conitin A., Cividini, A. and Gioda, G (2007), "Numerical evaluation of surface displacement of due to soil grouting and to tunnel excavation", *Int. J. Geomech.*, **7**(3), 217-226. https://doi.org/10.1061/(ASCE)1532-3641(2007)7:3(217).

Croce, P., Flora A. and Modoni, G. (2014), *Jet Grouting: Technology, Design and Control*, Taylor and Francis, London, New York.

Davis, E.N., Gunn, M.J., Mair, R.J. and Seneviratne, H.N. (1980), "The stability of shallow tunnels and underground openings in cohesive material", *Geotechnique*, **30**(4), 397-416. https://doi.org/10.1680/geot.1980.30.4.397.

Dutta, P. and Bhattacharya, P. (2019), "Stability of rectangular tunnels in cohesion less soil", *Int. J. Geotech. Eng*., **15**(10), 1345-1351. https://doi.org/10.1080/19386362.2019.1592874.

Fuente, M., Sulem, J., Taherzadeh, R. and Subrin D, (2019), "Tunneling in Squeezing ground: Effect of the excavation method", *Rock Mech. Rock Eng*., **53** 601-623. https://doi.org/10.1007/s00603-019-01931-4.

Ganeshan, V. and Yang, J.Y. (2009), "Jet grouting and its application", *Proceedings of International Symposium on Ground improvement Technologies and Case Histories*, Singapore, December.

Gavin, K., Wout, B., Kovacevic, M.S. and Dehass, K. (2019), "Investigation of remaining life of an immersed tunnel in Netherland", *Proceedings in Tunnels and Underground Cities: Engineering and Innovation Meet Archaeology and Art* Taylor and Francis, London, 4831-4838. http://doi.org/10.1201/9780429424441-512.

Khezri, N., Mohamad, H. and Fatahi, B. (2016), "Stability assessment of tunnel face in a layered soil using upper bound theorem of limit analysis", *Geomech. Eng.,* **11**(4), 471-492. http://doi.org/10.12989/gae.2016.11.4.471.

Kimura, T. and Mair, R.J. (1981), "Centrifuge testing of model tunnels in soft clay", *Proceedings of 10th International Conference of Soil Mechanics and Foundation Engineering,* Rotterdam, Netherlands.

Kitazume, M. and Terashi, M. (2013), The Deep Mixing Method*, Taylor & Francis*, London.

Lee, C.J., Wu, B.R., Chen, H.T. and Chiang, K.H. (2006), "Tunnel stability and arching effects during tunneling in soft clayey soil", *Tunn. Undergr. Sp. Tech.*, **21**(2), 119-132. https://doi.org/10.1080/19386362.2019.1592874.

Liu, W., Wu, Y., Zhao H., Xu., X. and Miao, L. (2021), "Deformation of subway tunnel induced by overcrossing jacked box tunnel", *Symmetry Journals* **13** 1-15. https://doi.org/10.3390/sym13101800

Lyamin, A.V., Jack, D.L. and Sloan, S.W. (2001), "Collapse analysis of square tunnels in cohesive–frictional soils", *Proceedings of the First Asian–Pacific Congress on Computational Mechanics, Sydney*, N.S.W., Australia, November.

Mair, R.J. (1979), "Centrifugal modelling of tunnel construction in soft clay", Ph.D. Thesis, University of Cambridge, Cambridge, U.K.

Pan, Y.T., Xiao, H.W., Lee, F.H. and Phoon, K.K. (2016), "Modified isotropic compression relationship for cement-admixed marine clay at low confining stress", *Geotech. Test. J.*, **39**(4), 695-702. https://doi:10.1520/GTJ20150147.

Pan, Y., Liu, Y., Tyagi, A., Lee, F.H. and Li, D.Q. (2020), "Model Independent strength reduction factor for effect of spatial variability on tunnels with improved soil surround", *Geotechnique*, **71**(5), 406-422. https://doi.org/10.1680/jgeot.19.P.056.

Pellegrino, G. and Adams, D.N. (1996), "The use of jet grouting to improve soft clays for open face tunnelling", *Proceedings of the 2nd Symposium on Geotechnical aspects of Underground Construction in Soft Ground*, Rotterdam, Netherlands.

Pellegrino, G. and Bruce, D.A. (1996), "Jet grouting for the solution of tunnelling problems in soft clays", *Grouting and deep mixing*, Netherlands.

Pham, V.V., Do, N.A. and Dias, D. (2021), "Sub rectangular tunnel behaviour under seismic loading", *Appl. Sciences*, **11**(21), 9909. https://doi.org/10.3390/app11219909.

Plaxis 2D Ultimate (Computer software), *Bentley Systems.*

Qui, J., Liu, H., Lai, H., Chen, J. and Wang, K. (2018), "Investigating long term settlement of a tunnel built over improved loessial foundation soil using jet grouting technique*", J. Perform. Constr. Fac.*, 04018066 1-15. https://doi.org/10.1061/(ASCE)CF.1943-5509.0001155.

Raju, V.R., Yohannes, M.M and Daramalinggam (2021), "The development of deep soil mixing practice and application in Malaysia", *Proceedings of the Deep foundation Institute Deep Soil Mixing - Online Conference 2021.*

Sloan, S.W. and Assadi, A. (1991), "Undrained stability of square tunnel in soil whose strength increases linearly with depth", *Comput. Geotech*., **12**, 321-346. https://doi.org/10.1016/0266-352X(91)90028-E.

Tan, T.S., Goh, T.L. and Yong, K.Y. (2002), "Properties of Singapore marine clays improved by cement mixing", *Geotech. Test. J.*, **25**(4), 422-433. https://doi.org 10.1520/GTJ11295J.

Terashi, M., Tanaka, H., Mitsumoto, T., Niidome, Y. and Honma, S. (1980), "Fundamental properties of lime and cement-treated soils", *Rep. PHRI*, **19**(1), 33-62 (in Japanese).

Terashi, M. and Tanaka, H. (1983), "Settlement analysis for deep mixing method", *Proceedings of the 8th European Conference on SMFE*, Vol. 2, A.A. Balkema, Rotterdam, Netherlands.

Tornaghi, R. and Cippo, A.P. (1985), *Soil Improvement by Jet Grouting for the Solution of Tunnelling Problems*, Institution of Mining ang metallurgy, London, United Kingdom.

Tyagi, A., Zulkefli, M.F.B., Pan Y., Goh, S.H. and Lee, F.H. (2017), "Failure modes of tunnel with improved soil surround", *J. Geotech. Geoenviron. Eng.*, **143**(11), 04017088, 1-13. https://doi.org/10.1061/(ASCE)GT.1943-5606.0001788.

Tyagi, A. and Lee, F. H (2017), "Factors affecting stability of large diameter tunnel in improved soil surround", *Proceedings of 19th*

International Conference on Soil mechanics and Geotechnical Engineering Seoul, South Korea, September

Tyagi, A., Liu, Y., Pan, Y.T., Ridhwan, K.B.M. and Lee, F.H. (2018), "Stability of tunnels in cement-admixed soft soils with spatial variability", *ASCE J. Geotech. Geoenviron. Eng.*, 06018012, 1-7. https://doi.org/10.1061/(ASCE)GT.1943-5606.0001988.

Tyagi, A., Wong, Y.C. and Lee, F.H (2019), "Effect of loading strain rates on peak strength and drainage behaviour of cement-treated clay", *Proceedings of the 16th Asian regional Conference on Soil Mechanics and Geotechnical Engineering*, Taipei, Taiwan, October.

Tyagi A., Liu Y., Pan Y.T. and Lee F.H. (2020), "Equivalent strength for tunnels in cement-admixed soil columns with spatial variability and positioning error", *ASCE J. Geotech. Geoenviron. Eng.*, **146**(10), 04020101, 1-13. https://doi.org/10.1061/(ASCE)GT.1943-5606.0002351.

Tyagi, A. and Lee, F.H. (2022), "Influence of tunnel failure on the existing large diameter tunnel in improved soil surround", *Tunn. Undergr. Sp. Tech*., **120**, 104247, 1-19. https://doi.org/10.1016/j.tust.2021.104276.

Tyagi, A. and Tamta, D. (2023), "Equivalent design strengths for spatially variable cement-treated soil slope", *Int. J. Geomech. ASCE*, article in production. https://doi.org/10.1061/IJGNAI/GMENG-8207.

Uktitchon, B. and Keawsawasvong, S. (2020), "Undrained stability of unlined square tunnel in clays with linearly increasing anisotropic shear strength", *Geotech. Geol. Eng.*, **38**, 897-915. https://doi.org/10.1007/s10706-019-01023-8.

Wang, Y.Q., Kong, W.K. and Wang, Z.F. (2018), "Effect of expanding rectangular tunnels on adjacent structures", *Adv. Civil Eng.*, 1729041. https://doi.org/10.1155/2018/1729041.

Wang, L., Kong, C., Peng, F., Zhang, B., Deng, J., Gu, S. and Sun, Q. (2020), "Construction of large-section long pedestrian underpass using pipe jacking in water filled clay", *Proceedings of the International conference on road tunnel safety and risk prevention and control*, Chongqing, China, December.

Wilson, D.W., Abbo, A.J., Sloan, S.W. and Yamamoto, K. (2017), "Undrained stability of rectangular tunnels where shear strength increases linearly with depth", *Can. Geotech. J.*, **54**(4), 469-480. https://doi.org/10.1139/cgj-2016-0072.

Xiao, H.W. (2009), "Yielding and failure of cement treated soil", Ph.D. Thesis, National University of Singapore, Singapore.

Yamamoto, K., Lyamin, A.V., Wilson, D.W., Sloan, S.W. and Abbo, A.J. (2011), "Stability of a circular tunnel in cohesive frictional soil subjected to surcharge loading", *Comput. Geotech.*, **38**(4), 504-514. https://doi.org/10.1016/j.compgeo.2011.02.014.

Yang, F. and Yang J.S. (2010), "Stability of shallow tunnel using rigid blocks and finite element upper bound solutions", *Int. J. Geomech*., **10**(6), 242-247. https://doi.org/10.1061/(ASCE)GM.1943-5622.0000011.

Yang, X.L. and Qin, C.B. (2014), "Limit analysis of rectangular cavity subjected to seepage forces based on Hoek-Brown failure criteria", *Geomech. Eng*., **6**(5) 503-515. https://doi.org/10.12989/gae.2014.6.5.503.

Yang, X.L. and Zhang, R. (2017), "Collapse analysis of shallow tunnel subjected to seepage in layered soil considering joined effect of settlement and dilation", *Geomech. Eng*., **13**(2), 217-235. https://doi.org/10.12989/gae.2017.13.2.217.

Yee, Y.W. and Tan, Y.C. (2015), "Excavation support for TBM retrieval shaft using deep soil mixing technique, Kuala Lumpur", *Proceedings of the International conference and exhibition on Tunneling and underground space*. Institute of Engineers Malaysia (IEM) Malaysia.

Zhang, J., Hang, Z., Feng, T. and Yang, F. (2020), "Assessment of the stability of an unlined rectangular tunnel with an overload on the ground surface", *Adv. Civil Eng.*, 6616067, 1-13. https://doi.org/10.1155/2020/6616067.

Zhao. H., Sun, H., Zhang, D. and Liu, C. (2021), "Mechanical properties of progressive failure characteristics of sandstone containing elliptical and square openings subjected to biaxial stress", *Plos One* **16**(3), 1-22. https://doi.org/10.1371/journal.pone.0246815.

Zulkefli, M.F.B., Tyagi, A. and Lee, F.H. (2017), "Collapse behaviour of large rectangular tunnel in improved soil surround", *Proceedings of the 9th International Symposium on Geotechnical Aspects of underground Construction in Soft Grounds (IS-São Paulo 2017)*, (Eds., A. Negro and M.O. Cecilio Jr.), CRC Press/Balkema, The Netherlands, April.

JS